RSC Advances

RSC Publishing

PAPER

View Article Online
View Journal | View Issue

# Nitro and amino BODIPYS: crucial substituents to modulate their photonic behavior†

Cite this: *RSC Advances*, 2013, **3**, 1547

Ixone Esnal,[a] Jorge Bañuelos,*[a] Iñigo López Arbeloa,[a] Angel Costela,[b] Inmaculada Garcia-Moreno,[b] Miguel Garzón,[c] Antonia R. Agarrabeitia[c] and María José Ortiz[c]

Received 15th November 2012,
Accepted 16th November 2012

DOI: 10.1039/c2ra22916a

**www.rsc.org/advances**

The present work deals with the synthesis and photophysical, quantum mechanical, and lasing characterization of novel BODIPYs bearing amino and nitro groups at different positions in the core. The results emphasize the relevant role on the photophysical and lasing properties, not only of the attached functionality but also of the position in which is grafted, as well as the molecular structure of the indacene core. A wide part of the visible spectrum can be covered by the insertion of an amino group at position 3 (red shift) or 8 (blue shift). Furthermore, the electron withdrawing character of the nitro substituent induces intramolecular charge transfer processes, the efficiency of which depends on the position of the nitro group on the BODIPY core. All these experimental findings can be rationalized with the help of quantum mechanical calculations.



## Introduction

The family of difluoroboradiazaindacenes, known by the trade name BODIPY, is currently considered as comprising some of the most useful and versatile fluorophores. The numerous applications of these compounds (biotechnology, electronics, *etc.*) require the design of new fluorophores with properties such as high stability, high fluorescence quantum yields, large Stokes shifts, and suitable absorption profiles, as well as incorporating substituents that optimize the function of these compounds in the different applications.[1] The incorporation of appropriate functional groups onto the chromophore could lead to new photophysical processes or large spectral shifts. Thus, the type of substituents and the position in which they are attached to the chromophore allow obtainment of, for example, a highly fluorescence dye in the red part of the visible spectrum or a system in which fluorescence properties are sensitive to a certain property of the surrounding environment. Therefore, one should choose carefully the kind of substituents and the position in which they will be incorporated to BODIPY, depending on the desired application.[1]

Post-modification of the BODIPY core is a convenient method for the facile functionalization of these dyes. The extensive literature available on BODIPY dyes shows that substitution at all positions has been investigated.[1–9] Several synthetic strategies have been used for this purpose, such as Knoevenagel-type condensation[1a–c,g,2] and oxidative formylation of methyl-substituted BODIPYs,[3] nucleophilic substitutions[1a–c,g,4] and palladium coupling reactions[1a,5] on halogenated BODIPYs, direct hydrogen substitution,[6] the Liebeskind–Srögl reaction[7] and electrophilic substitution reactions.[1a,8] Furthermore, the replacement of fluoride atoms by carbon and oxygen nucleophiles or by other halogen atoms has been shown to be an important advance for the introduction of functionality.[1a–c,2c,k,8b,9]

Functionalization at the 2,6-positions from 1,3,5,7-tetramethyl substituted BODIPYs can be achieved by electrophilic substitution reactions.[1a,8] Thus, halogenation at these positions has been extensively studied.[5f,8b–f] However, the nitration of BODIPYs has not attracted so much research interest as demonstrated by the few related publications in the literature. As we know, there is an example of nitration in the 2,6-positions of the commercial BODIPY core named PM546 (**A**),[10] and there are several Japanese patents with two dinitro derivatives (**B**[11] and **C**[12]), but neither their syntheses nor their spectroscopic data have been described (Fig. 1). Moreover, electrophilic substitution reactions in pyrrole-unsubstituted BODIPYs have attracted relatively little research interest until very recently[4h,8g–j] and, specifically, there is no study on the nitration reaction in this type of compound. In contrast, there are numerous examples of BODIPYs with nitro groups but not

[a]*Departamento de Química Física, Universidad País Vasco (UPV-EHU), Aptdo. 644, 48080, Bilbao, Spain*
[b]*Departamento de Sistemas de Baja Dimensionalidad, Superficies y Materia Condensada, Instituto Quimica-Fisica "Rocasolano", CSIC, Serrano 119, 28006 Madrid, Spain*
[c]*Departamento de Química Orgánica I, Facultad de Ciencias Químicas, Universidad Complutense, 28040, Madrid, Spain*

† Electronic Supplementary Information (ESI) available: details of the synthesis route, NMR spectra, photophysical data. See DOI: 10.1039/c2ra22916a

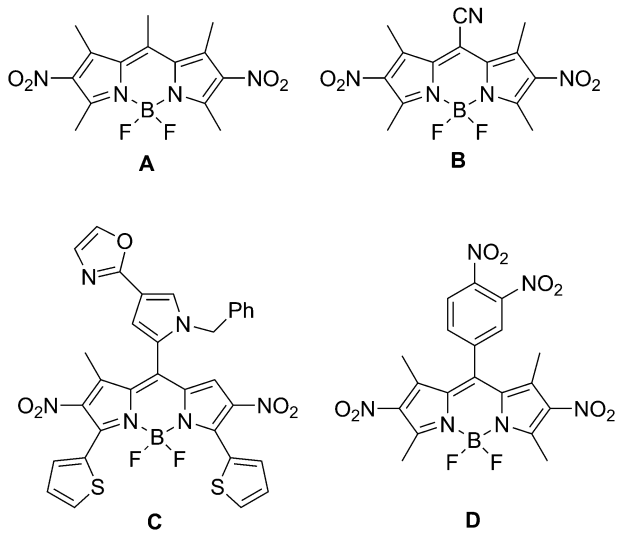


**Fig. 1** Chemical structures for 2,6-dinitro-1,3,5,7-substituted BODIPYs (**A**, **B** and **C**), and 8-dinitroaryl BODIPY (**D**).

directly attached to the BODIPY core (**D**),[1a,13] and most of them are used as precursors of amino groups (Fig. 1).

In this work we report the synthesis of new nitro derivatives of two different BODIPY scaffolds, by electrophilic substitution and subsequent reduction to the corresponding amino derivatives (Fig. 2). This library of new dyes allows us to analyze in detail the dependence of their optical properties on the nature and position of the substituents linked to a symmetric and asymmetric BODIPY core.

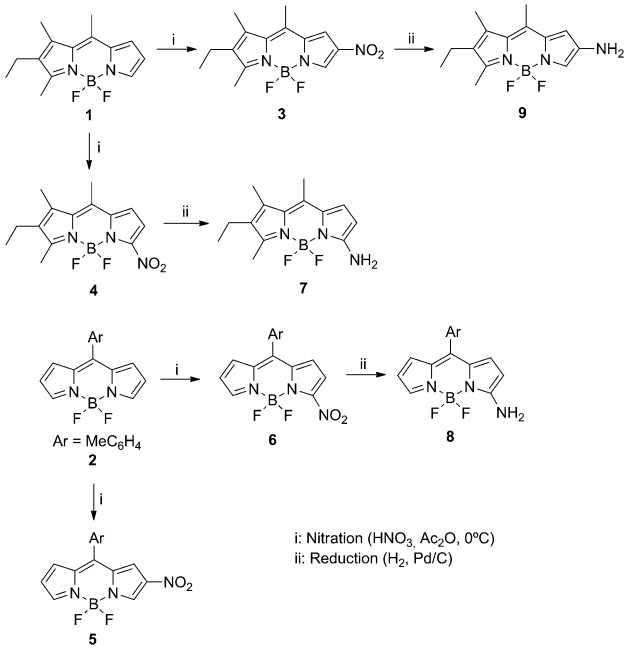


**Fig. 2** Starting BODIPYs (**1**, **2**) and core-nitro and amino BODIPY dyes (**3**–**9**) studied in this work.

Furthermore, the present work provides new insight into the effect of the molecular structure on the photophysical properties of the resulting chromophore. The nitration of BODIPYs induces new photophysical processes such as charge transfer phenomena, the influence on the optical properties of which is strongly dependent on the type of substituent, as well as the position where it is anchored to the chromophore. Therefore, the correct selection of functional groups and the most convenient position to graft them to the core allows the design of tailor-made BODIPY for the desired application, ranging from BODIPY covering a wide part of the visible part of the spectrum (amino substitution) to fluorophores sensitive to the environmental properties (nitro substitution). Moreover, these derivatives should be excellent scaffolds to further functionalization, leading to a wide battery of available structures based on BODIPY.

## Results and discussion

### Synthesis

Nitration of the BODIPY core has been carried out by electrophilic substitution reaction. Thus, the reaction of BODIPY dye **1**[14] with 2 equiv. $HNO_3$ in $Ac_2O$ at 0 °C gave a mixture of 6-nitro derivative **3** (11%) and 5-nitro derivative **4** (37%), which were separated *via* flash chromatography on silica. A similar result was obtained from pyrrole-unsubstituted BODIPY **2**[15] with 4 equiv. $HNO_3$ in $Ac_2O$, yielding 2-nitro derivative **5** (6%) and 3-nitro derivative **6** (36%). No other nitro BODIPY was formed under these reaction conditions. Increasing the amount of $HNO_3$ gave a complex mixture of nitro products.

Due to the low yields obtained from β-nitro derivatives **3** and **5**, we carried out the independent synthesis of these compounds from nitro pyrrole precursors (Scheme 1). Thus, the reaction of 2-acetyl-4-nitro-1*H*-pyrrole (**10**)[16] and 3-ethyl-2,4-dimethyl-1*H*-pyrrole with phosphorus oxychloride in $CHCl_3$, followed by treatment with $BF_3{\cdot}OEt_2$ in the presence of triethylamine, gave a moderate yield of BODIPY **3**. For the preparation of BODIPY **5**, we carried out the nitration of (1*H*-pyrrol-2-yl) (4-tolyl) methanone (**11**),[17] yielding a mixture of (5-nitro-1*H*-pyrrol-2-yl) (4-tolyl) methanone (**12**) and (4-nitro-1*H*-pyrrol-2-yl) (4-tolyl) methanone (**13**), which were separated *via* flash chromatography on silica. The condensation of compound **13** and pyrrole with phosphorus oxychloride, followed by treatment with $BF_3{\cdot}OEt_2$ in the presence of triethylamine allowed us to isolate BODIPY **5**, but, as in the direct nitration of BODIPY **2**, with a very low yield (Scheme 1). In addition, this compound was very unstable and its photophysical study was not possible. The amino BODIPYs **7** and **8** were readily obtained by reduction of the nitro to the amino group in the presence of molecular hydrogen and a solid catalyst with a quantitative good yield. However, BODIPY **9** could not be isolated because it decomposes quickly.

### Photophysical properties

The photophysical properties of the parent compound **1** have been previously analyzed as a function of the solvent nature.[14]

 

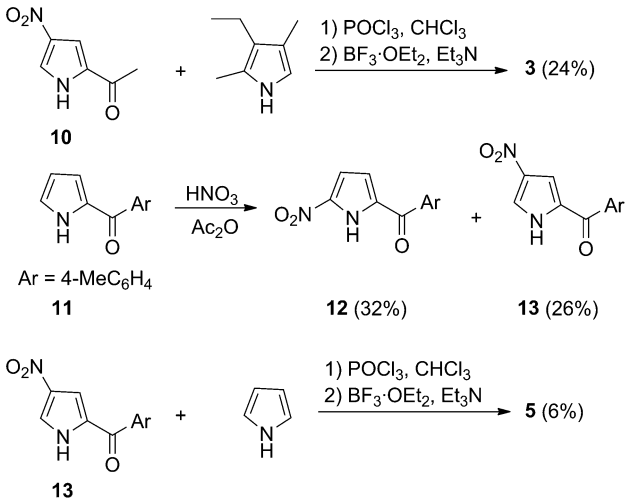


**Scheme 1** Independent synthesis of BODIPYs **3** and **5**.



Its photophysics were conditioned by the asymmetric substitution pattern, which reduces the absorption probability, while its fluorescence efficiency remained high, close to 100% in apolar solvents (Table 1). In addition, the asymmetric charge distribution in the pyrroles, induced by the substitution pattern, increased the non-radiative deactivation pathway and led to a moderate fluorescence quenching in polar media (around 25%), not reflected in the fluorescence lifetime. This behavior was a consequence of a concomitant decline in the radiative rate constant (parallel to the decrease in the molar absorption) and an enhancement of the non-radiative deactivation rate constants with the solvent polarity, which further favored the charge separation between the pyrrols.

**Amino substitution.** With respect to the parent dye **1**, the presence of an amino group at position 5 (compound **7**) red-shifts the spectral bands (around 20 nm), owing to the electron donor ability of the amine, which enhances the delocalized electronic density in the chromophoric core (Table 1 and Fig. 3, left). Similar red shifts have been reported for BODIPYs bearing amino groups at positions 3 and 5.[18] The 5-amino substituent increases the asymmetry in the charge distribution with the consequent decrease in the absorption probability of the new derivative **7**. Alternatively the fluorescence quantum yield remains high in apolar media, whereas it significantly decreases in polar media, following the same dependence on the solvent polarity to that previously observed for the reference dye **1** (Table 1). In fact, the electron releasing capacity of the amino at position 5 is not strong enough to induce a charge transfer state, which usually drastically quenches the fluorescence emission of BODIPYs. Theoretical simulations do not suggest an electronic density shift from the amino to the BODIPY core upon excitation, and the frontier orbital contour maps keep the normal features of the fluorophore, but extended to the amino group.

**Table 1** Photophysical properties of compound **1** and its 5-amino derivative (**7**) in apolar (cyclohexane) and polar media (methanol). The full photophysical data in other solvents are collected in Table S1 (ESI†)

| | $\lambda_{ab}$ (nm) | $\varepsilon_{max}$ ($M^{-1}$ $cm^{-1}$) | $\lambda_{fl}$ (nm) | $\varphi$ | $\tau$ (ns) |
|---|---|---|---|---|---|
| **1** | | | | | |
| c-Hexane | 504.0 | 33000 | 515.0 | 0.96 | 5.46 |
| Methanol | 495.5 | 25000 | 512.5 | 0.76 | 5.78 |
| **7** | | | | | |
| c-Hexane | 522.0 | 19000 | 538.0 | 0.97 | 4.44 |
| Methanol | 510.0 | 9000 | 534.0 | 0.74 | 4.54 |

The inclusion of the same group at position 6 (compound **9**) gave rise to a very unstable product, with fast degradation, losing the spectral bands typical of BODIPY. The electronic coupling of the amino at such a position could give rise to the formation of an emanine–imine tautomeric equilibrium (Scheme S1, ESI†) destroying the delocalized π-system of the chromophore. Therefore, entirely different results were obtained by changing the position in which the amino group was attached. Such a key role of the substitution position on the optical properties is reinforced by previous results reported by a BODIPY bearing just an amino group in the *meso* position.[7e,19] While the presence of this group in position 5 led to a slight bathochromic shift of the spectral bands, the substitution at position 8 induced a large blue shift (Fig. 3, right).

The reason for such opposite behavior can be understood through the theoretical simulation of the electronic distribution in the frontier orbitals involved in the corresponding spectral transition. With independence of the substitution, the electronic density at position 5 of the BODIPY core is nearly similar in the HOMO and LUMO states (Fig. 3). Thus, the 5-amino substituent only increased the delocalization of the π-system, red-shifting the spectral bands. However, the electronic density at position 8 of the BODIPY core increases significantly upon excitation from the HOMO to the LUMO state, highlighting the *meso* position as being very sensitive to substituent effects. Then, the electron donor amine linked at the 8-position raised up the energy of the LUMO state, leaving the HOMO state unaltered,[19] and, consequently, leading to an increase of the energy gap, which is reflected in the blue-shift of the spectral bands.

**Nitro substitution.** Following an opposite behavior to that previously described for amino substitution, the presence of a nitro group at position 5 (compound **4**) as well as at 6 (compound **3**) gave rise to a hypsochromic shift of the absorption band due to its electron withdrawing character (Fig. 4), which removes part of the electronic density delocalized through the BODIPY core. Nonetheless, the most striking feature induced by nitro substitution is a drastic change in the shape of both the absorption and fluorescence spectra. Indeed, the absorption bands seem to be split into two transitions, behavior that becomes clearer in fluorescence, where very broad emission bands were registered.

Taking into account the strong electron-withdrawing character of the substituent, one could wonder that this photophysical behavior is related to the presence of an intramolecular charge transfer (ICT) state, active even in the ground state. However, the influence of the ICT on the spectral bands is not well defined, since absorption transitions attributed to ICT have been reported as red-shifted and as blue-shifted, with respect to the locally excited (LE) state.[20]

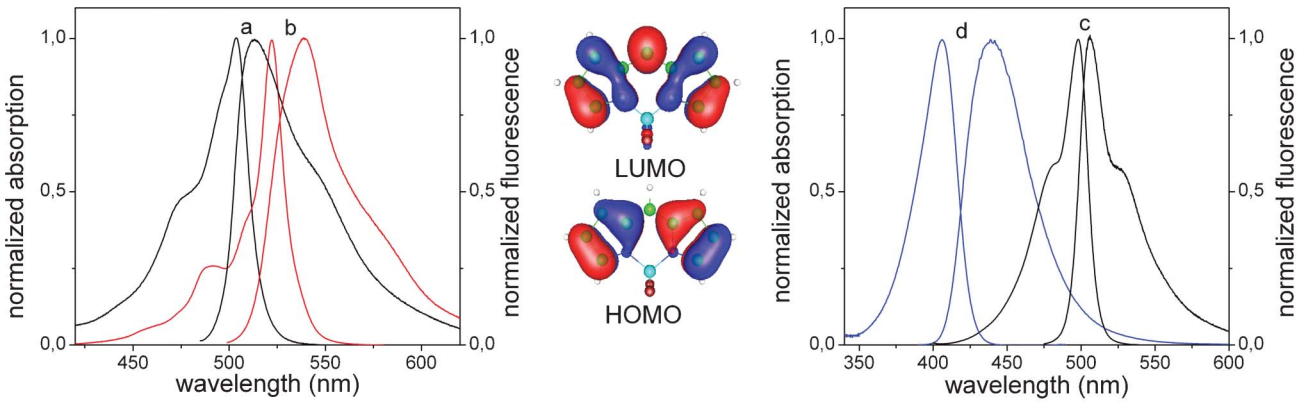


**Fig. 3** (Left) Absorption and fluorescence spectra of the alkylated BODIPY **1** (a) and its 5-amino substituted derivative **7** (b). (Right) For comparison purposes, the corresponding spectral bands of the fully unsubstituted BODIPY dye (named as BDP) and its 8-amino derivative ((c) and (d), respectively)[7c,19] are included. For the sake of clear understanding of the opposite spectral shifts induced by the amino group depending on the grafting position, the HOMO and LUMO contour maps of the BODIPY core are also included.

More clearly perceptible is the dependence of the ICT states on the solvent nature, since they are stabilized in polar media due to their high dipole moment. Thus, their spectral bands are very sensitive to the solvent polarity and usually show large Stokes shifts in polar solvents.

However, the spectra of these nitro derivatives are characterized by small Stokes shifts and low solvatochromism. Indeed, the presence of such a possible second band becomes less evident in polar media, whereas the spectral transitions involving ICT states usually appear clearer, as the polarity of the solvent increases. Moreover, the fluorescence spectra and fluorescence decay curves of these nitro-substituted BODIPYs do not change with the excitation wavelength (or emission wavelength in the later case), and also their excitation spectra perfectly match the absorption ones, regardless of the emission wavelength. All this evidence allows rejection of the hypothesis of the presence of an ICT state as the origin of the apparent spectral splitting, which could be more related to the change in the vibrational structure of the bands induced by the nitro group, because of the following features: (a) the vibrational resolution appears clearer in apolar media; (b) there is only one emitting entity, since the spectral bands and the decay curves are independent of the excitation and emission wavelengths; (c) the solvatochromism of the spectra is quite low (see Fig. S1 in the ESI†), and (d) theoretical simulation of the absorption spectrum only predicts one transition in the visible region.

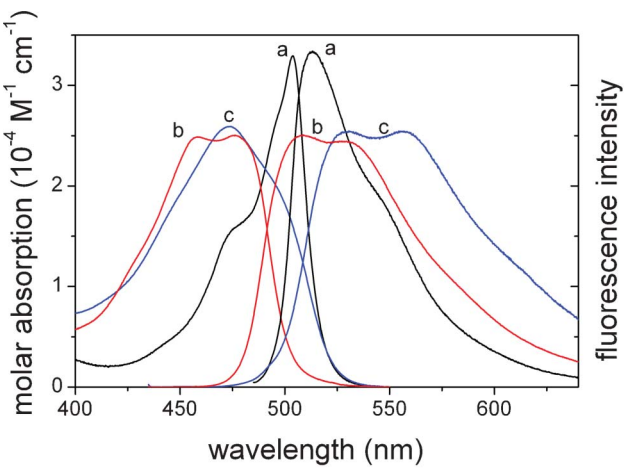


**Fig. 4** Absorption and fluorescence spectra of compound **1** (a) and its nitro derivatives **3** (b) and **4** (c).

Regarding the fluorescence properties, the presence of the nitro group reduced the fluorescence efficiency and the lifetime of the BODIPY, as shown in Table 2 and Fig. 5. Such a decrease was more evident in polar media, where the fluorescence decay is faster. This trend is more dramatic in compound **4**, because in the most polar media the fluorescence ability becomes negligible and the corresponding decay curve has to be deconvoluted as biexponential, with a dominating short lifetime (around 50 ps in methanol). The marked sensitivity of the fluorescence quantum yield and decay curve on the solvent polarity can be related to the presence of an extra non-radiative deactivation pathway in these media.

Taking into account the strong electron-withdrawing ability of the nitro group, the reason for the fluorescence quenching should be an ICT state, built up from the LE state. The presence of an ICT has been discussed before to explain the shape of the spectra. Although such a hypothesis was discarded as an explanation of the spectral splitting, it does not mean that the ICT is not taking place in the excited state. From the above discussion, it is clear that the ICT state is not formed in the ground state. Nonetheless, it can be populated in the excited state, but with absence of self-emission, which allows the maintenance of the vibrational resolution of the absorption spectrum in the fluorescence one. Therefore, the formation of an ICT state upon excitation in the nitro derivatives **3** and **4** explains the decrease in fluorescence ability. Generally, the ICT states are characterized by a poor or negligible emission, since they are placed at lower energies than the LE state and non-radiative deactivation is more

 

**Table 2** Photophysical properties of reference compound **1** and its nitro derivatives (**3** and **4**) in cyclohexane and methanol. The full photophysical data in several solvents are listed in Table S2 (ESI†)

| | $\lambda_{ab}$ (nm) | $\varepsilon_{max}$ ($M^{-1}$ $cm^{-1}$) | $\lambda_{fl}$ (nm) | $\varphi$ | $\tau$ (ns) | $k_{fl}$ ($10^{-8}$ $s^{-1}$) | $k_{nr}$ ($10^{-8}$ $s^{-1}$) |
|---|---|---|---|---|---|---|---|
| c-Hexane | | | | | | | |
| **1** | 504.0 | 33000 | 515.0 | 0.96 | 5.46 | 1.75 | 0.07 |
| **3** | 458.0 | 24000 | 509.0 | 0.53 | 3.13 | 1.70 | 1.49 |
| | 476.0 | 24000 | 530.0 | | | | |
| **4** | 474.0 | 25000 | 530.5 | 0.17 | 1.53 | 1.11 | 5.42 |
| | | | 556.0 | | | | |
| Methanol | | | | | | | |
| **1** | 495.5 | 25000 | 512.5 | 0.76 | 5.78 | 1.31 | 0.41 |
| **3** | 446.5 | 21000 | 509.5 | 0.17 | 1.54 | 1.10 | 5.39 |
| | | | 526.5 | | | | |
| **4** | 462.5 | 20000 | 530.5 | 0.005 | 0.05 (91%) | — | — |
| | | | | | 1.73 (9%) | | |

feasible. In fact, in some derivatives, the ICT emission is weakly detected in non-polar media. The ICT stabilization in polar media implies a loss of its fluorescence emission, because the consequent red-shift favors the non-radiative deactivation from the ICT state.[20a] Moreover, the charge transfer could be as feasible as a ''dark'' charge separation (CS) state could be populated from the ICT state. In this state the charge transfer is so high that the charges are fixed and the electronic delocalization is stopped, hence contributing further to the loss of fluorescence emission.

The fluorescence quenching ability of the ICT state induced by the nitro group depends on the chromophoric position at which it is attached. In fact, its inclusion at position 5 led to a more drastic decrease in the fluorescence efficiency and lifetime than at position 6. Generally, in BODIPYs the dipole moment is located along the transversal axis with the positive charge density placed around the central position 8 and the negative charge density at the fluorine atoms (Fig. 6). Thus, the charge separation should be more effective upon incorporation of an electron acceptor group (nitro) at the bottom part of the BODIPY (position 5, compound **4**) than at the rest of the positions (*i.e.*, position 6, compound **3**). In fact, the presence of the nitro substituent significantly increases the theoretically calculated dipole moment of the molecule, from 6.6 D of the parent compound **1** to 11.6 D for derivative **3** and up to 12.8 D for compound **4** (Fig. 6). These results indicate that the quenching effect of the ICT is more important in the derivative **4** where, in polar media, the fluorescence almost disappears (<0.01). Moreover, in this last derivative the decay curve becomes biexponential, with a main component characterized by a very fast lifetime (around 50 ps), which is attributed to the quenching of the fluorescence LE state by the ICT state, and a residual contribution of a lifetime around 1.5–2 ns, resembling that of the LE state. In more polar solvents such as 2,2,2-trifluoroethanol, the fluorescence quantum yield decreases, making an accurate deconvolution of the corresponding decay curve impossible.

Consequently, the nitro derivatives described herein work as polarity sensors due to the ICT state. They do not represent good laser dyes but, apart from being excellent starting points for further functionalization, they are very sensitive to the environmental polarity.

**Amino and nitro derivatives of 8-tolyl BODIPY 2.** The photophysics of the reference compound 2 are controlled by the presence of the phenyl ring in the *meso* position. The absence of substituents at adjacent positions enables free rotation of the aryl group. Such a motion greatly increased the internal conversion process, owing to vibrational couplings, causing a drastic decrease of the BODIPY fluorescence ability ($\varphi < 0.05$ and $\tau < 400$ ps; see Table S3, ESI†). Moreover,

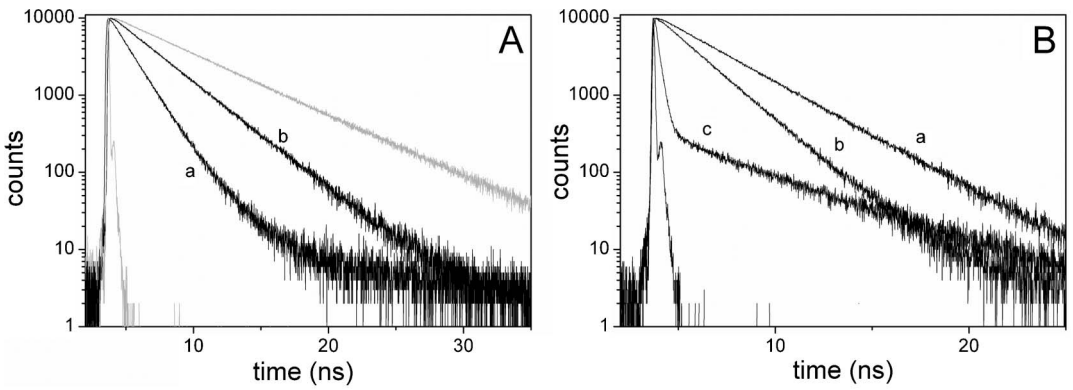


**Fig. 5** (A) Fluorescence decay curve of compound **1** (grey) and its nitro derivatives **3** (b) and **4** (a) in cyclohexane. (B) Decay curves of compound **2** as a function of the solvent; cyclohexane (a), acetone (b) and $F_3$-ethanol (c).

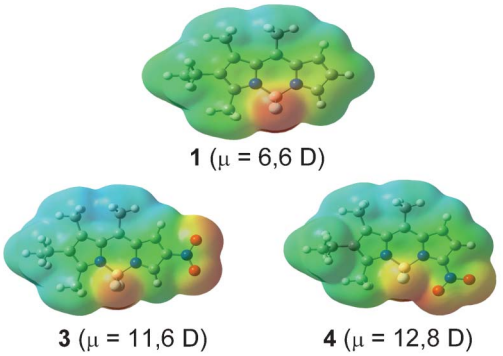


**Fig. 6** Electrostatic potential mapped onto the electronic density for compound **1** and its nitro derivatives **3** and **4**. The corresponding calculated dipole moments are also included.

interaction between the phenyl and indacene electronic clouds could not be discarded and could further take part in the non-radiative deactivation processes.[21]

While the presence of an amine at position 5 in asymmetric compound **1** (dye 7) led to a bathochromic spectral shift and kept the high fluorescence ability of the BODIPY, the presence of such a group in the 8-tolyl-BODIPY core (compound **8**) gave completely opposite results: a slight hypsochromic shift and a lower fluorescence efficiency ($\varphi < 0.03$ and $\tau < 150$ ps; see Table S3, ESI†). Therefore, in this case, the electron releasing ability of the amine substituent increases the non-radiative deactivation processes. This donor resonant effect should increase the electronic charge at the BODIPY core, and hence, the deleterious effect in fluorescence of the phenyl free motion should be more important than in the above amino derivatives without such an 8-aryl group. The molecular orbitals of compound **8**, depicted in Fig. 7, show that transition from the HOMO to the LUMO state implies a shift of electronic density from the amino-BODIPY core to the phenyl ring. Considering the electron donor character of the amine and the ability of the phenyl group to behave as donor or acceptor depending on its substitution, the additional presence of a quenching ICT state should be operative. Indeed, in the most acidic media (2,2,2-trifluoroethanol), where the amine can be protonated and its electron donor ability should be lower, the highest fluorescence quantum yield is achieved, in concordance with a lower formation probability of the ICT state.

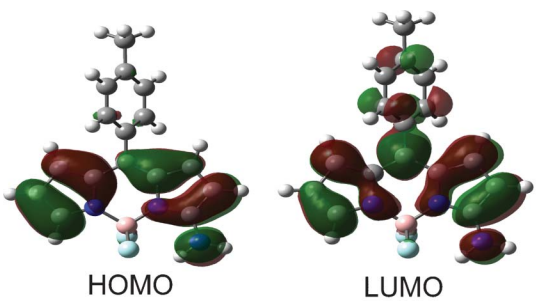


**Fig. 7** HOMO and LUMO contour maps of compound **8**.

The vibrational resolution of the spectral bands upon nitration of the reference 8-tolyl-BODIPY (compound **6**) was not so marked as previously observed in the nitro derivatives of compound **1**. In this case, the spectral bands are similar to that shown by BODIPY dyes (see Fig. S2, ESI†), although they became broader in polar media. Once more, these features confirm that the nitro group tends to alter the vibrational resolution of the electronic transitions, and reinforce the above interpretation of the absence of spectral bands from any ICT state for derivative **6**, as well for **3** and **4**.

Surprisingly, whereas the nitration of alkyl BODIPY was very harmful to the fluorescence efficiency, the nitration of the 8-tolyl-BODIPY at position 5 (compound **6**) ameliorates the fluorescence ability of the chromophore (Fig. 8). The electron withdrawing character of the nitro group removes electronic density from the chromophore, including from the central position. Thus, the effect of the aryl free motion is reduced and the fluorescence efficiency is somewhat recovered.

The essential role of the electron character of the substituent in the fluorescence ability of derivatives bearing bulky groups with free motion should be noted. Taking into account the fact that the internal conversion processes have been associated with the structural rigidity/flexibility, the electron donor moieties (*i.e.* amine) increase the negative influence of such rotational freedom on the fluorescence while the electron acceptor ones (*i.e.* nitro) counteract this non-radiative pathway. To this aim, the most effective positions to be substituted are 3 and 5 (beginning and end of the delocalized π-system of the BODIPY).[8j,15]

Following a similar behavior to that previous described and discussed for the nitro derivatives **3** and **4**, in the case of compound **6**, the electron withdrawing effect of the nitro group was so high that, in the more polar environments, the mentioned ICT state is more stabilized and effectively quenches its fluorescence emission (Fig. 8). In fact, the fluorescence quantum yield of dye **6** in methanol clearly

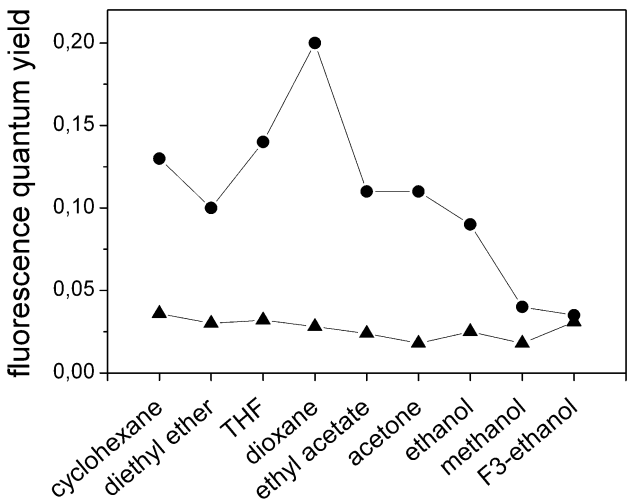


**Fig. 8** Evolution of the fluorescence quantum yield of reference compound **2** (triangles) and its nitro derivative **6** (circles) in several solvents ordered by their polarity.

drops, to values as low as those of the reference compound **2**, and, simultaneously, the lifetime becomes shorter (around 500 ps in methanol, Table S3, ESI†). It should be mentioned that the decay curve of the nitro-derivative **6** is described as monoexponential even in polar media, while the nitration of compound **1** at the same position 5 (compound **4**) gave rise to a biexponential decay in polar solvents. Such behaviour should be related to the inherent high internal conversion probability induced by the aryl free motion in the derivatives of compound **2**, which reduces the influence of the ICT process in the fluorescence decay of dye **6**.

### Lasing properties

The position of the absorption bands of the derivatives with amino substitution allows for studying their lasing properties under pumping at 532 nm. Under our experimental conditions (transversal excitation and strong focusing of the incoming pump radiation, see experimental section), the concentration of the dyes in the different solvents for the lasing studies should be in the millimolar range, so that the incoming pump radiation penetrates the sample (*i.e.* is absorbed) to a depth similar to that of the thickness of the pump stripe at the input face of the cell onto which the pumping radiation is focused (about 0.3 mm). This gives rise to an emitted beam with a near-circular cross-section and optimizes the lasing efficiency (ratio between the energy of the dye laser output and the pump energy incident on the sample surface).

Compound **9**, where the amino group was at position 6, was very unstable, as discussed above, when dealing with its photophysical properties, and its lasing behavior could not be characterized. Thus, only the lasing properties of compound **7**, with the amino group at position 5, could be studied. Although the highest fluorescence quantum yield of this compound was obtained in cyclohexane (Table S1, ESI†), it could not be dissolved in this apolar solvent at the concentrations required to obtain laser emission. Thus, the dependence of the laser emission on the concentration of the solvent was studied in ethyl acetate, which was the solvent where compound **7** exhibits the next highest quantum yield. It was found (Table 3) that the optimum concentration was $1.4 \times 10^{-3}$ M, rendering a lasing efficiency of 29%. Lower and higher concentrations resulted in decreased lasing efficiency. This behavior of the emission efficiency is typical of lasing dyes. The lasing efficiency first increases with dye concentration up to a point from where further increases in concentration result in a decrease in the lasing efficiency, due to the increase in reabsorption/re-emission processes. The growing importance of reabsorption/re-emission processes with dye concentration is also reflected in the progressive red-shift of the wavelength of the laser emission.

In Table 3 are also presented the efficiency and peak wavelength of the laser emission of compound **7** in polar aprotic and polar protic solvents at the determined optimum dye concentration. The lasing efficiencies correlate well with the dye photophysical properties in diluted solutions (Table S1, ESI†): the higher the fluorescence quantum yield, the higher the lasing efficiency, with the lowest efficiency being obtained in polar protic solvents. In this regard, it should be indicated than no laser emission was observed when the solvent was 2,2,2-trifluoroethanol.

Due to the hypsochromic shift of the absorption bands in the nitro derivatives, their lasing properties were first studied under pumping at 355 nm, which is the usual pump wavelength for dyes emitting in the blue spectral region. Once again, although the highest fluorescence quantum yields of the nitro derivatives **3** and **4** were obtained in apolar solvent cyclohexane, these compounds could not be dissolved in this solvent at the high concentrations needed for laser operation under the transversal pumping arrangement.

Compound **4** did not exhibit laser action, even under our drastic pumping conditions, which was to be expected taking into account the low fluorescence efficiency of this dye in all solvents (see Table S2, ESI†). Compound **3** did exhibit laser action, albeit with efficiencies of less than 10% under the 355 nm pumping (Table 4). From Table S2, ESI,† and Fig. 3, it is seen that although the absorption bands of the nitro derivatives are blue shifted, away from the typical pump wavelength of 532 nm, the shift is not enough to move the bands as far away as 355 nm, so that absorption at this wavelength is rather low. Higher lasing efficiency would be expected if the nitro derivatives are pumped at or near the maximum of their absorption bands. Thus, we used a Coumarin 460-based dye laser, working at 450 nm (see experimental section), to pump compound **3** at the peak of its absorption band. As can be seen in Table 4, under these conditions the lasing efficiency of this compound in ethyl acetate doubled to 18%. This lasing efficiency is still lower than those obtained with the amino derivatives (Table 3), as is to be expected given the lower fluorescence quantum yields of

**Table 3** Maximum wavelength of the laser emission ($\lambda_{la}$) and lasing efficiency (Eff) of compound **7** as a function of the concentration in ethyl acetate and in different solvents at a given concentration. Pump wavelength was 532 nm

| Solvent | $c$ (mM) | $\lambda_{la}$ (nm) | Eff (%) |
|---|---|---|---|
| Ethyl acetate | 0.8 | 563 | 24 |
| | 1.4 | 564 | 29 |
| | 1.9 | 568 | 20 |
| | 2.8 | 568 | 14 |
| Methanol | 1.4 | 558 | 12 |
| Acetone | 1.4 | 573 | 20 |
| DCM | 1.4 | 576 | 23 |

**Table 4** Maximum wavelength of the laser emission ($\lambda_{la}$) and lasing efficiency (Eff) of compound **3** as a function of the concentration in ethyl acetate and in different solvents at a given concentration

| Solvent | $\lambda_{pump}$[a] (nm) | $c$ (mM) | $\lambda_{la}$ (nm) | Eff (%) |
|---|---|---|---|---|
| Ethyl acetate | 355 | 2.2 | 534 | 9 |
| | 355 | 4.5 | 539 | 7 |
| | 355 | 6.7 | 540 | 4 |
| Ethyl acetate | 450 | 2.2 | 537 | 11 |
| | 450 | 4.5 | 538 | 18 |
| | 450 | 6.7 | 540 | 16 |
| Acetone | 450 | 4.5 | 534 | 8 |
| Methanol | 450 | 4.5 | 539 | 5 |

[a] $\lambda_{pump}$: pump wavelength.

compound **3** with respect to those of compound **7** (Tables S1 and S2, ESI†). When compound **3** is dissolved in acetone or methanol its lasing efficiency decreases, in good correlation with the photophysical properties (lower fluorescence quantum yields in these solvents than in ethyl acetate).

The 8-tolyl BODIPYs, derivatives of compound **2** with amino or nitro groups at position 4 (compounds **8** and **6**, respectively), have very low fluorescence quantum yields (Table S3, ESI†) in all solvents and, correspondingly, their laser emission was very inefficient. Under 355 nm pumping and at the optimum concentration of $2 \times 10^{-3}$ M, compound **8** lased at 550 nm with an efficiency of just 1%, whereas compound **6**, which has somewhat higher fluorescence quantum yields, emitted laser radiation at 563 nm with an efficiency of 4%.

## Conclusion

The present work highlights the essential role of the nature and position of the substituent, as well as the molecular structure of the indacene core, in the optical properties of BODIPYs. In this sense, the same functional group may lead to entirely opposite results, just by varying the position in which it is incorporated to the chromophore and/or the molecular structure of the core. The amine group at position 3 led to a modest red shift, but the same group at position 8 led to a large hypsochromic shift. On the other hand, the strong withdrawing character of the nitro group induced intramolecular charge transfer processes in the excited state, where the quenching effect over the fluorescence emission depends strongly on the position in which it is added to the indacene core. In spite of this, laser action has been demonstrated in both amine and nitro derivatives, with lasing properties exhibiting good correlation with the photophysical properties.

Furthermore, the amino and nitro derivatives described herein are excellent precursors, from a synthetic point of view, to design BODIPY derivatives with different functionalizations.

## Experimental section

### Materials

Starting materials and reagents used in the preparation of BODIPYs are commercially available. The solvents were dried and distilled before use.

### Synthesis of BODIPY 1–9

BODIPY dyes **1**[14] and **2**[15] were synthesized by the methods previously described. These compounds were transformed in the corresponding nitro BODYPYs **3–6** by treatment with $HNO_3/Ac_2O$. By means of a catalytic hydrogenation over Pd on charcoal, the nitro derivatives **4** and **6** can be easily reduced to the corresponding amino BODIPYs **7** and **8**. The syntheses and spectroscopic data for all compounds are described in the ESI.†

### Characterization of the new dyes

Spectral data of the known compounds were in accordance with the literature data. Flash column chromatography was performed using silica gel Merck 60 (230–400 mesh). $^1$H and $^{13}$C NMR spectra were recorded with a Bruker Avance-DPX-300 spectrometer (300 MHz for $^1$H and 75 MHz for $^{13}$C) and a Bruker Avance III spectrometer (700 MHz for $^1$H and 176 MHz for $^{13}$C). Chemical shift multiplicities are reported as s = singlet, d = doublet, t = triplet, q = quartet and m = multiplet. IR spectra (in $cm^{-1}$) were recorded in a Bruker Tensor-27-FTIR spectrophotometer. Melting points were determined in open capillaries and are uncorrected. High resolution mass spectra were determined by ESI (electrospray ionization) in a FTMS Bruker APEX Q IV and by EI (electron impact) in a Thermofisher MAT 95 XP (see ESI†).

### Photophysical properties

The photophysical properties were registered in dilute solutions (around $2 \times 10^{-6}$ M), prepared by adding the corresponding solvent to the residue from the adequate amount of concentrated stock solution in acetone, after vacuum evaporation of this solvent. UV-Vis absorption and fluorescence spectra were recorded on a Varian model CARY 4E spectrophotometer and a SPEX Fluorolog 3-22 spectrofluorimeter, respectively. The fluorescence spectra were corrected from the wavelength dependence of the detector sensibility. The fluorescence quantum yield ($\varphi$) was obtained using a methanolic solution of PM567 as a reference ($\varphi^r$=0.91). Radiative decay curves were registered with the time correlated single-photon counting technique (Edinburgh Instruments, model FL920) using a microchannel plate detector (Hamamatsu C4878), with picosecond time resolution ($\sim$20 ps). Fluorescence emission was monitored at the maximum emission wavelength after excitation at 410, 440 and 470 nm by means of a diode laser (PicoQuant, model LDH410, 440 and 470, respectively) with 150 ps FWHM pulses. The fluorescence lifetime ($\tau$) was obtained from the slope after the deconvolution of the instrumental response signal from the recorded decay curves by means of an iterative method. The closeness of the exponential fit was controlled by statistical parameters (chi-square, Durbin–Watson and the analysis of the residuals). The radiative ($k_{fl}$) and non-radiative deactivation ($k_{nr}$) rate constants were calculated by means of: $k_{fl} = \varphi/\tau$ and $k_{nr} = (1 - \varphi)/\tau$, respectively.

### Laser experiments

Liquid solutions of dyes were contained in 1 cm optical-path length cells, which were carefully sealed to avoid solvent evaporation during the experiments. The dye solutions were transversely pumped with nanosecond pulses either at 532 nm (6 ns FWHM and 5.5 mJ/pulse) or at 355 nm (8 ns FWHM and 3.5 mJ/pulse). The source of the 532 nm pulses was a frequency-doubled Q-switched Nd:YAG laser (Monocrom OPL-10). The 355 nm pulses were the third harmonic of a Q-switched Nd:YAG laser (Spectron SL282G). In both cases the excitation pulses were line-focused onto the cell, providing pump fluences on the active medium of 180 mJ $cm^{-2}$ and 110 mJ $cm^{-2}$ for 532 nm and 355 nm pumping, respectively. The

 

oscillation cavity (2 cm in length) consisted of a 90% reflectivity back aluminum mirror and the lateral face of the cell as an output coupler. Experiments were also performed at a pump wavelength of 450 nm, with 12 ns, 3 mJ pulses from a dye laser (ethanolic solution of Coumarin 460 pumped with the Spectron SL282G 355 nm pulses). The energy of dye and pump laser pulses was measured with GenTec ED-100A and ED-200 pyroelectric energy meters. The spectral characteristics of the laser emission were determined by collecting a fraction of the emission by an optical fiber attached to the input slit of a spectrograph/monochromator (SpectraPro-300i, Acton Research Corporation) equipped with a charge-coupled device (CCD)/SpectruMM:GS 128B).



## Acknowledgements

This work was supported by Projects MAT2010-20646-C04-01, -02 and -04 and TRACE 2009-0144 of the Spanish Ministerio de Economía y Competitividad (MINECO). Ixone Esnal thanks the Gobierno Vasco for predoctoral contracts (S-PE10UN65, SPE11UN064, SPE12UN140 and IT339-10)

## References

1 (*a*) A. Loudet and K. Burgess, *Chem. Rev.*, 2007, **107**, 4891–4932; (*b*) R. Ziessel, G. Ulrich and A. Harriman, *New J. Chem.*, 2007, **31**, 496–501; (*c*) G. Ulrich, R. Ziessel and A. Harriman, *Angew. Chem., Int. Ed.*, 2008, **47**, 1184–1201; (*d*) F. L. Arbeloa, J. Bañuelos, V. Martinez, T. Arbeloa and I. L. Arbeloa, *Trends Phys. Chem.*, 2008, **13**, 101–122; (*e*) A. C. Benniston and G. Copley, *Phys. Chem. Chem. Phys.*, 2009, **11**, 4124–4131; (*f*) M. Benstead, G. H. Mehl and R. W. Boyle, *Tetrahedron*, 2011, **67**, 3573–3601; (*g*) N. Boens, V. Leen and W. Dehaen, *Chem. Soc. Rev.*, 2012, **41**, 1130–1172.

2 (*a*) K. Rurack, M. Kollmannsberger and J. Daub, *Angew. Chem., Int. Ed.*, 2001, **40**, 385–387; (*b*) O. Buyukcakir, O. A. Bozdemir, S. Kolemen, S. Erbas and E. U. Akkaya, *Org. Lett.*, 2009, **11**, 4644–4647; (*c*) O. A. Bozdemir, R. Guliyev, O. Buyukcakir, S. Selcuk, S. Kolemen, G. Gulseren, T. Nalbantoglu, H. Boyaci and E. U. Akkaya, *J. Am. Chem. Soc.*, 2010, **132**, 8029–8036; (*d*) T. Bura, P. Retailleau and R. Ziessel, *Angew. Chem., Int. Ed.*, 2010, **49**, 6659–6663; (*e*) S. Kolemen, O. A. Bozdemir, Y. Cakmak, G. Barin, S. Erten-Ela, M. Marszalek, J.-H. Yum, S. M. Zakeeruddin, M. K. Nazeeruddin, M. Grätzel and E. U. Akkaya, *Chem. Sci.*, 2011, **2**, 949–954; (*f*) T. Bura, P. Retailleau, G. Ulrich and R. Ziessel, *J. Org. Chem.*, 2011, **76**, 1109–1117; (*g*) O. A. Bozdemir, S. Erbas-Cakmak, O. O. Ekiz, A. Dana and E. U. Akkaya, *Angew. Chem., Int. Ed.*, 2011, **50**, 1–7; (*h*) H. He, P.-C. Lo, S.-L. Yeung, W.-P. Fong and D. K. P. Ng, *Chem. Commun.*, 2011, **47**, 4748–4750; (*i*) T. Bura, D. Hablot and R. Ziessel, *Tetrahedron Lett.*, 2011, **52**, 2370–2374; (*j*) N. Boens, W. Qin, M. Baruah, W. M. De Borggraeve, A. Filarowski, N. Smisdom, M. Ameloot, L. Crovetto, E. M. Talavera and J. M. Alvarez-Pez, *Chem.–Eur. J.*, 2011, **17**, 10924–10934; (*k*) S. Zhu, J. Zhang, G. Vegesna, A. Tiwari, F.-T. Luo, M. Zeller, R. Luck, H. Li, S. Green and H. Liu, *RSC Adv.*, 2012, **2**, 404–407; (*l*) J.-H. Olivier, J. Barberá, E. Bahaidarah, A. Harriman and R. Ziessel, *J. Am. Chem. Soc.*, 2012, **134**, 6100–6103; (*m*) C. W. Evans, M. J. Latter, D. Ho, S. A. M. A. Peerzade, T. D. Clemons, M. Fitzgerald, S. A. Dunlop and K. S. Iyer, *New J. Chem.*, 2012, **36**, 1457–1462.

3 A. Haefele, C. Zedde, P. Retailleau, G. Ulrich and R. Ziessel, *Org. Lett.*, 2010, **12**, 1672–1675.

4 (*a*) T. Rohand, M. Baruah, W. Qin, N. Boens and W. Dehaen, *Chem. Commun.*, 2006, 266–268; (*b*) L. Li, B. Nguyen and K. Burgess, *Bioorg. Med. Chem. Lett.*, 2008, **18**, 3112–3116; (*c*) Ö. Dilek and S. L. Bane, *Tetrahedron Lett.*, 2008, **49**, 1413–1416; (*d*) E. Fron, E. Coutiño-Gonzalez, L. Pandey, M. Sliwa, M. Van der Auweraer, F. C. De Schryver, J. Thomas, Z. Dong, V. Leen, M. Smet, W. Dehaen and T. Vosch, *New J. Chem.*, 2009, **33**, 1490–1496; (*e*) W. Qin, V. Leen, W. Dehaen, J. Cui, C. Xu, X. Tang, W. Liu, T. Rohand, D. Beljonne, B. Van Averbeke, J. N. Clifford, K. Driesen, K. Binnemans, M. Van der Auweraer and N. Boens, *J. Phys. Chem. C*, 2009, **113**, 11731–11740; (*f*) L. Jiao, C. Yu, M. Liu, Y. Wu, K. Cong, T. Meng, Y. Wang and E. Hao, *J. Org. Chem.*, 2010, **75**, 6035–6038; (*g*) L. Jiao, C. Yu, T. Uppal, M. Liu, Y. Li, Y. Zhou, E. Hao, X. Hu and M. G. H. Vicente, *Org. Biomol. Chem.*, 2010, **8**, 2517–2519; (*h*) V. Leen, T. Leemans, N. Boens and W. Dehaen, *Eur. J. Org. Chem.*, 2011, **23**, 4386–4396; (*i*) O. Dilek and S. L. Bane, *J. Fluoresc.*, 2011, **21**, 347–354; (*j*) M. Zhang, E. Hao, J. Zhou, C. Yu, G. Bai, F. Wang and L. Jiao, *Org. Biomol. Chem.*, 2012, **10**, 2139–2145; (*k*) X. Li, S. Huang and Y. Hu, *Org. Biomol. Chem.*, 2012, **10**, 2369–2372; (*l*) G. Ulrich, A. Haefele, P. Retailleau and R. Ziessel, *J. Org. Chem.*, 2012, **77**, 5036–5048.

5 (*a*) T. Rohand, W. Qin, N. Boens and W. Dehaen, *Eur. J. Org. Chem.*, 2006, 4658–4663; (*b*) W. Qin, T. Rohand, W. Dehaen, J. N. Clifford, K. Driesen, D. Beljonne, B. Van Averbeke, M. Van der Auweraer and N. Boens, *J. Phys. Chem. A*, 2007, **111**, 8588–8597; (*c*) S. Rihn, P. Retailleau, N. Bugsaliewicz, A. De Nicola and R. Ziessel, *Tetrahedron Lett.*, 2009, **50**, 7008–7013; (*d*) R. Guliyev, A. Coskun and E. U. Akkaya, *J. Am. Chem. Soc.*, 2009, **131**, 9007–9013; (*e*) O. A. Bozdemir, Y. Cakmak, F. Sozmen, T. Ozdemir, A. Siemiarczuk and E. U. Akkaya, *Chem.–Eur. J.*, 2010, **16**, 6346–6351; (*f*) M. J. Ortiz, I. Garcia-Moreno, A. R. Agarrabeitia, G. Duran-Sampedro, A. Costela, R. Sastre, F. López Arbeloa, J. Bañuelos Prieto and I. López Arbeloa, *Phys. Chem. Chem. Phys.*, 2010, **12**, 7804–7811; (*g*) C. Thivierge, J. Han, R. M. Jenkins and K. Burgess, *J. Org. Chem.*, 2011, **76**, 5219–5228; (*h*) T. K. Khan and M. Ravikant, *Tetrahedron*, 2011, **67**, 5816–5824; (*i*) Y. Wu, X. Ma, J. Jiao, Y. Cheng and C. Zhu, *Synlett*, 2012, **23**, 778–782.

6 (*a*) C. Thivierge, R. Bandichhor and K. Burgess, *Org. Lett.*, 2007, **9**, 2135–2138; (*b*) J. Chen, M. Mizumura, H. Shinokubo and A. Osuka, *Chem.–Eur. J.*, 2009, **15**, 5942–5949; (*c*) V. Leen, V. Zaragozí Gonzalvo, W. M. Deborggraeve, N. Boens and W. Dehaen, *Chem. Commun.*, 2010, **46**, 4908–4910; (*d*) V. Leen, M. Van der Auweraer, N. Boens and W. Dehaen, *Org. Lett.*, 2011, **13**, 1470–1473; (*e*) B. Verbelen, V. Leen, L. Wang, N. Boens and W. Dehaen, *Chem. Commun.*, 2012, **48**, 9129–9131.

7 (*a*) T. V. Goud, A. Tutar and J.-F. Biellmann, *Tetrahedron*, 2006, **62**, 5084–5091; (*b*) E. Peña-Cabrera, A. Aguilar-Aguilar, M. González-Domínguez, E. Lager, R. Zamudio-

Vázquez, J. Godoy-Vargas and F. Villanueva-García, *Org. Lett.*, 2007, **9**, 3985–3988; (*c*) J. Han, O. Gonzalez, A. Aguilar-Aguilar, E. Peña-Cabrera and K. Burgess, *Org. Biomol. Chem.*, 2009, **7**, 34–36; (*d*) E. Lager, J. Liu, A. Aguilar-Aguilar, B. Z. Tang and E. Peña-Cabrera, *J. Org. Chem.*, 2009, **74**, 2053–2058; (*e*) C. F. A. Gómez-Durán, I. García-Moreno, A. Costela, V. Martín, R. Sastre, J. Bañuelos, F. López Arbeloa, I. López Arbeloa and E. Peña-Cabrera, *Chem. Commun.*, 2010, **46**, 5103–5105; (*f*) I. J. Arroyo, R. Hu, B. Z. Tang, F. I. López and E. Peña-Cabrera, *Tetrahedron*, 2011, **67**, 7244–7250.

8 (*a*) L. Li, J. Han, B. Nguyen and K. Burgess, *J. Org. Chem.*, 2008, **73**, 1963–1970; (*b*) L. Bonardi, G. Ulrich and R. Ziessel, *Org. Lett.*, 2008, **10**, 2183–2186; (*c*) Ö. A. Bozdemir, O. Büyükcakir and E. U. Akkaya, *Chem.–Eur. J.*, 2009, **15**, 3830–3838; (*d*) K. Krumova and G. Cosa, *J. Am. Chem. Soc.*, 2010, **132**, 17560–17569; (*e*) S. Rihn, M. Erdem, A. De Nicola, P. Retailleau and R. Ziessel, *Org. Lett.*, 2011, **13**, 1916–1919; (*f*) R. P. Sabatini, T. M. McCormick, T. Lazarides, K. C. Wilson, R. Eisenberg and D. W. McCamant, *J. Phys. Chem. Lett.*, 2011, **2**, 223–227; (*g*) C. Yu, L. Jiao, H. Yin, J. Zhou, W. Pang, Y. Wu, Z. Wang, G. Yang and E. Hao, *Eur. J. Org. Chem.*, 2011, 5460–5468; (*h*) L. Jiao, W. Pang, J. Zhou, Y. Wei, X. Mu, G. Bai and E. Hao, *J. Org. Chem.*, 2011, **76**, 9988–9996; (*i*) Y. Hayashi, S. Yamaguchi, W. Y. Cha, D. Kim and H. Shinokubo, *Org. Lett.*, 2011, **13**, 2992–2995; (*j*) M. J. Ortiz, A. R. Agarrabeitia, G. Duran-Sampedro, J. Bañuelos Prieto, T. Arbeloa Lopez, W. A. Massad, H. A. Montejano, N. A. García and I. Lopez Arbeloa, *Tetrahedron*, 2012, **68**, 1153–1162.

9 (*a*) A. Harriman, L. Mallon and R. Ziessel, *Chem.–Eur. J.*, 2008, **14**, 11461–11473; (*b*) T. W. Hundnall, T.-P. Lin and F. P. Gabbaï, *J. Fluorine Chem.*, 2010, **131**, 1182–1186; (*c*) J.-H. Olivier, A. Haefele, P. Retailleau and R. Ziessel, *Org. Lett.*, 2010, **12**, 408–411; (*d*) C. A. Wijesinghe, M. E. El-Khouly, J. D. Blakemore, M. E. Zandler, S. Fukuzumi and F. D'Souza, *Chem. Commun.*, 2010, **46**, 3301–3303; (*e*) T. Bura and R. Ziessel, *Org. Lett.*, 2011, **13**, 3072–3075; (*f*) X.-D. Jiang, J. Zhang, T. Furuyama and W. Zhao, *Org. Lett.*, 2012, **14**, 248–251; (*g*) T. Lundrigan, S. M. Crawford, T. S. Cameron and A. Thompson, *Chem. Commun.*, 2012, **48**, 1003–1005.

10 M. Shah, K. Thangaraj, M.-L. Soong, L. T. Wolford, J. H. Boyer, R. Politzer and T. G. Pavlopoulos, *Heteroat. Chem.*, 1990, **1**, 389–399.

11 T. Suzuki, T. Tanaka, I. Higashiguchi and A. Oda, *JP Patent 11176572*, 1999.

12 K. Takuma, T. Misawa, K. Sugimoto, T. Nishimoto, H. Tsukahara and K. Takuma, *JP Patent 10273504*, 1998.

13 T. Tachikawa, N. Wang, S. Yamashita, S.-C. Cui and T. Majima, *Angew. Chem., Int. Ed.*, 2010, **49**, 8593–8597.

14 J. Bañuelos Prieto, A. R. Agarrabeitia, I. Garcia-Moreno, I. Lopez-Arbeloa, A. Costela, L. Infantes, M. E. Perez-Ojeda, M. Palacios-Cuesta and M. J. Ortiz, *Chem.–Eur. J.*, 2010, **16**, 14094–14105.

15 A. Cui, X. Peng, J. Fan, X. Chen, Y. Wu and B. Guo, *J. Photochem. Photobiol., A*, 2007, **186**, 85–92.

16 H. Oda, T. Hanami, T. Iwashita, M. Kojima, M. Itoh and Y. Hayashizaki, *Tetrahedron*, 2007, **63**, 12747–12753.

17 A. R. Katritzky, K. Suzuki, S. K. Singh and H.-Y. He, *J. Org. Chem.*, 2003, **68**, 5720–5723.

18 W. Qin, V. Leen, T. Rohand, W. Dehaen, P. Dedecker, M. Van der Auweraer, K. Robeyns, L. Van Meervelt, D. Beljonne, B. Van Averbeke, J. N. Clifford, K. Driesen, K. Binnemans and N. Boens, *J. Phys. Chem. A*, 2009, **113**, 439–447.

19 J. Bañuelos, V. Martin, C. F. A. Gómez-Durán, I. J. Arroyo-Córdoba, E. Peña-Cabrera, I. García-Moreno, A. Costela, M. E. Pérez-Ojeda, T. Arbeloa and I. López Arbeloa, *Chem.–Eur. J.*, 2011, **17**, 7261–7270.

20 (*a*) M. Kollmannsberger, K. Rurack, U. Resch-Genger and J. Daub, *J. Phys. Chem. A*, 1998, **102**, 10211–10220; (*b*) Z. R. Grabowski, K. Rotkiewicz and W. Rettig, *Chem. Rev.*, 2003, **103**, 3899–4032; (*c*) W. Qin, M. Baruah, M. Van der Auweraer, F. C. De Schryver and N. Boens, *J. Phys. Chem. A*, 2005, **109**, 7371–7384.

21 H. L. Kee, C. Kirmaier, L. Yu, P. Thamyongkit, W. J. Youngblood, M. E. Calder, L. Ramos, B. C. Noll, D. F. Bocian, W. E. Scheidt, R. R. Birge, J. S. Lindsey and D. Holten, *J. Phys. Chem. B*, 2005, **109**, 20433–20443.

 